

# Many-body localization regime for cavity induced long-range interacting models

Titas Chanda<sup>1</sup> and Jakub Zakrzewski<sup>2,3,\*</sup>

<sup>1</sup>The Abdus Salam International Centre for Theoretical Physics (ICTP), Strada Costiera 11, 34151 Trieste, Italy

<sup>2</sup>Institute of Theoretical Physics, Jagiellonian University, Lojasiewicza 11, 30-348 Kraków, Poland

<sup>3</sup>Mark Kac Complex Systems Research Center, Jagiellonian University, Lojasiewicza 11, 30-348 Kraków, Poland.

Many-body localization (MBL) features are studied here for a large spin chain model with long range interactions. The model corresponds to cold atoms placed inside a cavity and driven by an external laser field with long range interactions coming from rescattering of cavity photons. Earlier studies were limited to small sizes amenable to exact diagonalization. It is shown that nonergodic features and MBL may exist in this model for random disorder as well as in the presence of tilted potential on experimental time scales also for experimentally relevant system sizes using tensor networks algorithms.

## I. INTRODUCTION

The pioneering works [1–3] started a modern area of intensive investigations of the interplay between the disorder and interactions. The belief that interacting closed systems inherently locally thermalize led to the eigenstate thermalization hypothesis (ETH) [4, 5]. On the other hand, the many-body localization (MBL) [1–3] became a prominent example of ETH breaking; – various aspects of MBL are discussed in recent reviews [6–10]. The strong believe in the existence of MBL phase in the thermodynamic limit (even a proof of it was proposed for a certain class of spin chains [11, 12]) was shattered by an influential recent contribution [13], which was followed by a number of works providing arguments for and against the existence of MBL in the thermodynamic limit [14–22]. Similar conclusions could be obtained from approximate time dynamics for large system sizes [23–26]. In effect, recent claims do suggest the separation of the physical picture into the finite time, finite size, experimentally reachable “MBL regime” leaving the question of the existence of the “MBL phase” in the strict thermodynamic regime open [27–29].

These works concentrate mainly on spin-1/2 systems with nearest neighbor interactions. Experimental signatures of MBL have been mainly seen for spinful fermions in cold optical lattices [30–33]. Bosons have also been theoretically considered [34, 35] – with a slight disadvantage due to a large effective local Hilbert space.

An early natural question has been posed whether MBL may be observed for long-range interactions. The pioneering experiment with effective Ising-type interactions has been realized in ion chain quantum simulator [36]. Several works have discussed the conditions on long-range tunnelings or interactions necessary for observing MBL, often concentrating on the relation between the power-law decay of the couplings  $\sim 1/|i-j|^\alpha$  (with  $i, j$  denoting lattice sites) and localization properties [37–41]. The lack of existence of MBL is postulated for  $\alpha < 2d$  with  $d$  being the dimension of the system on the basis

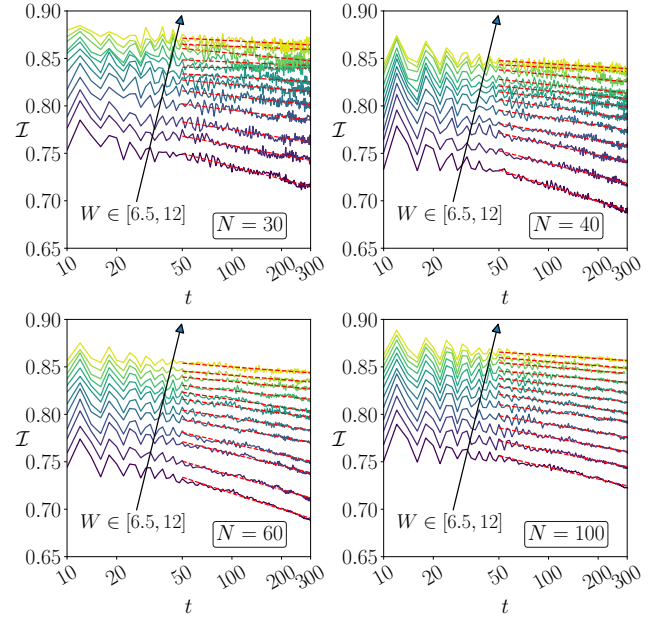


Figure 1. Imbalance as a function of time for different system sizes indicated in the panels and the all-to-all interaction strength  $U_1 = 1$ . The color codes different disorder amplitudes  $W$  (the higher  $W$  the slower the decay – highest lying curves correspond to the biggest  $W$  as indicated by the arrow pointing towards the direction of larger  $W$ s). Dashed red lines yield power law,  $t^{-\beta}$ , fits to the tails of the decay.

of perturbation type arguments. Actually, for isotropic interactions – as is the case studied below – the limit is much weaker,  $\alpha + 2 < 2d$  [37, 38] for a discussion see [41].

Surprisingly, recent works [42, 43] have shown that signatures of MBL may be observed in a certain type of infinitely-ranged interacting Hamiltonians representing atoms interacting both via contact and cavity-mediated interactions. The model considered consists of a one-dimensional (1D) atomic gas in an optical cavity and driven by an external laser field. Photon rescattering leads then to effective infinitely-ranged interactions corresponding to the equality in  $\alpha + 2 = 2d$  for one dimensional system. While [42] considered both fermions and bosons MBL in such a set-up with an imposed random-

\* jakub.zakrzewski@uj.edu.pl

diagonal disorder, one may consider also quasi-random interactions resulting from the mismatch between the wavelength of the external drive and the cavity [43].

Both these studies have considered small system sizes amenable to the exact diagonalization. The question naturally arises whether MBL will exist also for larger sizes, especially due to being at the edge of the localization condition [41]. Naturally, we cannot address the strict thermodynamic limit (and as seen from the discussion above, such a limit is controversial even for much simpler short-range interactions) but the modest question we want to address in this paper is whether the signatures of MBL can be observed for experimental sizes and time scales as realized in cavity experiments [44–48]. Contrary to the experiments, we shall limit ourselves to a 1D model [42] and use the state-of-the-art tensor network (TN) techniques [49–51] to study the time dynamics from appropriately prepared initial states. This is a long time established technique for “experimental” approach to MBL following the pioneering work [30].

The paper is organized as follows. First we briefly recall the model and study the time dynamics in the presence of random disorder. Later we consider localization in disorder-free tilted lattice that extends extensive recent studies of such models [52–58] to infinite range potentials. Let us also note here the recent work [59] which discusses localization in tilted lattice for dipolar i.e., power-law decaying interactions.

## II. MODEL AND METHODS

We consider cold spin-polarized fermions in a 1D optical lattice placed along a cavity axis. The cavity mode wavelength coincides with that of the laser forming the optical lattice. The optical lattice is sufficiently deep to facilitate a tight binding description of the system limited to its lowest band. In addition atoms scatter the laser light shined at them from the side. In the limit when cavity field may be adiabatically eliminated from the problem, as studied often both experimentally and theoretically [44, 47, 60–65] (for a broad reviews see [66, 67]), the Hamiltonian of the problem reads (see [42] for a recent derivation):

$$H_0 = \sum_{i=1}^{L-1} \left[ \frac{J}{2} (\hat{f}_i^\dagger \hat{f}_{i+1} + \text{c.c.}) + V \hat{n}_i \hat{n}_{i+1} \right] - \frac{U_1}{L} \sum_{i \neq j}^L (-1)^{i+j} \hat{n}_i \hat{n}_j \quad (1)$$

with  $\hat{f}_i$  being the annihilation operator for a fermion at site  $i$ ,  $\hat{n}_i = \hat{f}_i^\dagger \hat{f}_i$ ,  $L$  is the number of sites,  $J$  describes the hopping between sites and  $V$  is the strength of the contact interactions.  $U_1$  is the strength of cavity-mediated infinite range interactions, the scaling with the system size in the last term above assures that the Hamiltonian (1), is extensive in the large  $L$  limit.

The standard Jordan-Wigner transformation puts the Hamiltonian into Heisenberg spin chain formulation (for  $J = V = 1$  assumed as the energy unit later on) with infinite range interactions due to cavity induced term

$$H_0 = \sum_{i=1}^{L-1} \vec{S}_i \cdot \vec{S}_{i+1} - \frac{U_1}{L} \sum_{i \neq j}^L (-1)^{i+j} S_i^z S_j^z \quad (2)$$

where  $\vec{S}_i$  is 1/2-spin at site  $i$ . The system is modified by an additional random diagonal disorder term  $H_r = \sum_{i=1}^L h_i \hat{n}_i$  (corresponding to  $H_r = \sum_{i=1}^L h_i S_i^z$  in the spin language) where  $h_i$  are the random variables with uniform distribution in  $[-W, W]$  interval. The full Hamiltonian becomes:

$$H = H_0 + H_r. \quad (3)$$

We shall also consider the disorder free situation in Sec. IV where  $h_i$  becomes a simple function of the position. Specifically we consider a tilted lattice,  $h_i = Fi$  with  $F$  being the magnitude of the tilt, or we assume that  $h_i$  comes from the harmonic trapping potential. We consider a half filling case with  $L/2$  fermions (which corresponds to the largest spin sector  $\sum S_i^z = 0$ ) and consider time evolution of the initial charge-density wave Fock-like separable states. However, contrary to standard MBL approaches for short range interactions where, following experiments [30, 32], the Néel state  $|\psi(0)\rangle = |1, 0, 1, 0, \dots\rangle$  ( $|\uparrow, \downarrow, \uparrow, \downarrow, \dots\rangle$  in the spin language) is often assumed, we need a different strategy. For short range interactions and random disorder the model exhibits, in finite size studies, a mobility edge [68], the state  $|\psi(0)\rangle$  being most difficult to localize, making it a good candidate as a probe of dynamics. This is no longer true in the presence of all-to-all interactions with non-negligible  $U_1$  – the  $(-1)^{i+j}$  factor in the last term of (2) shifts the Néel state either close to the bottom or to the top (depending on the sign of  $U_1$ ) of the spectrum. Thus, to probe the system, we consider a sample of random initial separable Fock-like states that we choose to lay in the middle of the spectrum. For each realization of the disorder we find states of minimal and maximal energy by density matrix renormalization group (DMRG) algorithm [69, 70] and consider random states with energy close to the middle energy (see [25] for the details about the description of choosing the initial state near a given energy).

The numerical study of time dynamics is carried out using Time Dependent Variational Principle (TDVP) in the tensor network approach [51, 71–73], with an implementation based on the Itensor library [74] that has been thoroughly tested in our earlier works on short-ranged interacting systems [22, 75]. The diagonal all-to-all interaction term is efficiently represented as a matrix-product-operator enabling studies of realistic system sizes for times corresponding to typical times in cold-atoms time-dynamics experiments [76]. The time dynamics is addressed following the time evolution of the correlation

function

$$\mathcal{I}(t) = \frac{4}{L} \sum_{i=1}^L \langle S_i^z(t) \rangle \langle S_i^z(0) \rangle \quad (4)$$

which for a Néel state would reduce to a standard imbalance of occupations between odd and even states.

### III. THE DISORDERED CASE

Let us consider first a random uniform disorder. Fig. 1 shows the characteristic time dynamics of the “imbalance” or magnetization correlation function (4) for different system sizes  $L$  and for a non-negligible all-to-all interaction strength  $U_1 = 1$ . After a rapid initial decay from  $\mathcal{I}(0) = 1$  on a time scale of few hopping times (not shown) the long time dynamics is clearly dependent on the disorder amplitude  $W$ . The red dashed lines are approximate power-law  $\mathcal{I}(t) \sim t^{-\beta}$  fits that work remarkably well. That resembles similar observations for short range interacting models [24, 25, 32, 77]. On the other hand, comparing the disorder amplitudes for which data are obtained, a careful reader will notice that the slowdown of the dynamics and possible saturation of the imbalance occurs for much stronger disorder than for corresponding disordered Heisenberg spin chain [23, 24] where such a saturation is observed around  $W \approx 4 - 5$ .

We must stress that a determination of the disorder amplitude which may be considered as a border value for localization is notoriously difficult [22–24, 77]. For small system sizes, the algebraic decay observed after a rapid initial decrease of imbalance eventually slows down at long times – the imbalance reaches a final non-zero value (for a sufficiently large disorder) well beyond the Heisenberg time [22]. Such long times are unreachable for larger system sizes as Heisenberg time increases exponentially with the system size. Moreover, the current experimental capabilities limit the coherent, decoherence-free evolution in cold atoms to few hundreds of the tunneling time. Therefore, as the study of the evolution gets limited in time, one is forced to define a critical value of the power-law exponent  $\beta_c$  below which we may consider the system to be localized. One of the possibilities to get a correct estimate of  $\beta_c$  is to again refer to small systems and define  $\beta_c$  equal to the power-law exponent that occurs for such a disorder for which the level statistics is already close to be Poissonian indicating localization [24]. This leads to  $\beta_c \approx 0.02$  for short-ranged model. The other possible way is to adopt the criterion that vanishing  $\beta$  within error bars – coming from averaging over the disorder realizations – is sufficient [23] so that  $\beta_c$  becomes comparable with the standard deviation  $\sigma$  of  $\beta$ . For a sample of few hundreds of disorder realizations for  $L = 16$  as in [23], this leads, taking  $\beta_c = \sigma$ , to  $\beta_c \approx 0.01$  for short-ranged model. We adopt the same criterion of  $\beta_c = 0.01$  for simplicity.

To support this approach further, we provide a more quantitative comparison of the saturation by fitting the

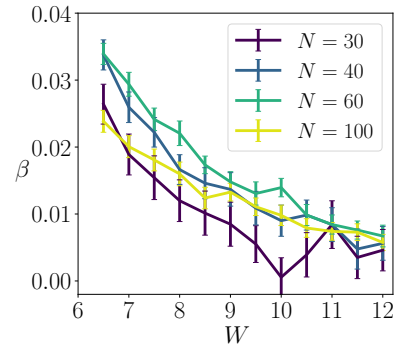


Figure 2. The average power-law decay of the imbalance for different system sizes. Here we plot the power-law exponent  $\beta$  as a function of the disorder strength  $W$  for different system sizes. The critical  $\beta = 0.01$  is reached around  $W = 10.5$ .

the power-law to the data for different system sizes as summarised in Fig. 2. While some system size dependence is still observed despite reaching  $L = 100$ ,  $\beta$  clearly decays with  $W$ . The adopted critical  $\beta_c = 0.01$  value is reached around  $W \approx 10.5$ . We note that the obtained value of the critical  $W$  estimated in this way quite nicely corresponds to that obtained via a finite size scaling of exact diagonalization results [42].

The work [42] have shown that the localization crossover point is strongly dependent on  $U_1$ . To see whether this conclusion persists for larger system sizes we fix the system size at  $L = 40$  and inspect the time dynamics for few values of  $U_1$ , c.f., Fig. 3. We again observe that the long time dynamics (here we extend our studies to 300 tunneling times, the value reachable with our algorithm for  $L = 40$ ) is well approximated by power-law behavior for different values of  $U_1$ . Then we can estimate the crossover to a localized model for different  $U_1$ , see Fig. 4. We observe that the stronger  $U_1$  (in the small interval studied) the bigger  $W$  are needed to reach the localization border, again in good agreement with results of [42] obtained for much smaller system sizes.

At this point let us comment that our numerical results does not provide any information about the thermodynamic limit in the problem studied. Even for short-range interacting systems this remains an open question (see e.g., [14, 16–18, 22, 29, 78, 79]). We merely show that for realistic system sizes and experimentally reachable evolution times the dynamics of the Hamiltonian (1) is strongly nonergodic and, for sufficiently strong  $W$ , shows localized behavior.

### IV. DISORDER-FREE MODELS

Consider now the second, already announced in Sec. II choice of  $h_i$  in  $H_r$  which becomes a smooth function of the site index. To be specific consider first  $h_i = Fi$  where  $F$  is a constant tilt of the lattice realized, e.g., [76] by the Zeeman effect. Without the optical cavity the model

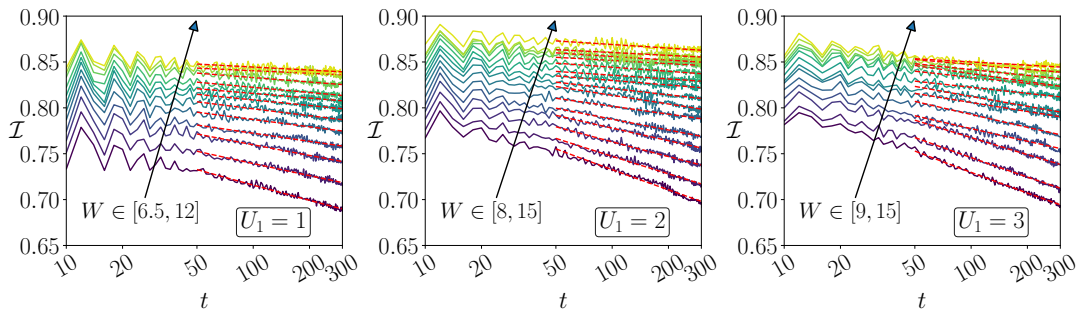


Figure 3. Imbalance as a function of time for different all-to-all interaction strength  $U_1$  and different, color coded disorder amplitudes  $W$  (as in Fig. 1) for the system size  $L = 40$ . Dashed red lines indicate power law fits to the data.

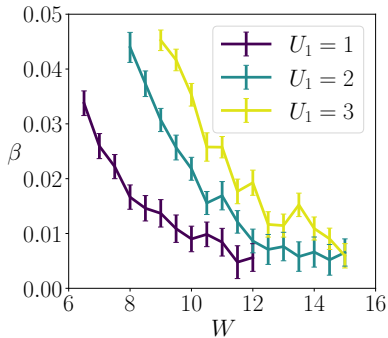


Figure 4. Fitted values of  $\beta$  for  $L = 40$  and different  $U_1$  values. The localization crossover shifts to larger disorder for stronger all-to-all interactions  $U_1$ .

(3) reveals the so called Stark many-body localization (SMBL) which has been intensively studied since its discovery for spinless fermions [52, 53] as well as for bosons [54, 58, 80], the experimental verification came with spinful fermions in optical lattice [76] as well as in quantum simulators [81–83]. It has been also studied for open systems [84]. Here we briefly consider whether the presence of the long-range cavity induced interactions affects SMBL.

For the Heisenberg spin chain the transition to SMBL is observed in dynamical studies for  $F$  of the order of unity. Here we consider larger values of  $F$  and show that the short time dynamics is characterized by the time scale inversely proportional to  $F^2$ , c.f., Fig. 5, in a similar manner to that observed for short-range Hamiltonians [58] and explained there by a pair tunneling mechanism that preserves the approximate global dipole moment,  $\mathcal{D} = \sum_i (i - i_0) f_i^\dagger f_i$ . Note that, for convenience, we evaluate the dipole moment with respect to the center of the system, where  $i_0$  is half-integer for even number of sites considered. The dipole moment preserving second order process corresponds to a tunneling of one particle by one site to the left while the other by one site to the right and is given by an effective tunneling rate  $\tilde{J} = 2VJ^2/F^2$  in the absence of all-to-all interactions [58] (for a detailed discussion of processes occurring at large  $F$  values

see [54]). The presence of all-to-all interactions affects slightly this picture. The second order pair tunneling process has now contributions with slightly different energies:

$$\tilde{J} = \frac{J^2}{-F - V - k_1 U_1/L} + \frac{J^2}{F - V - k_2 U_1/L} \approx \frac{J^2 [2V + (k_1 + k_2) U_1/L]}{F^2}, \quad (5)$$

where  $k_1$  and  $k_2$  are small positive or negative integers giving the energy difference due to all-to-all interactions for the corresponding single particle jump. Since  $U_1/L \ll V$  the additional terms proportional to  $k_i$  may be to a large extent neglected – see, however, below.

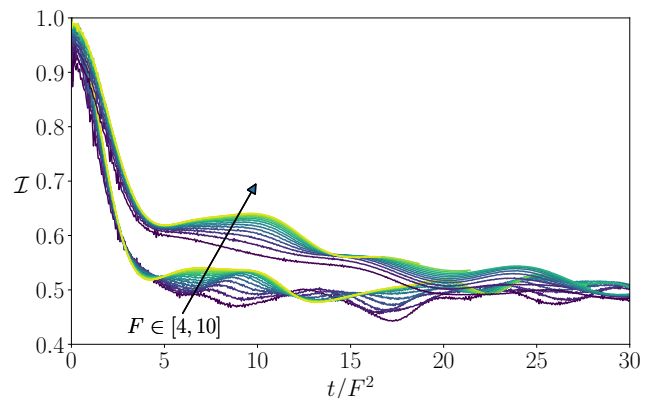


Figure 5. The time dynamics of the imbalance for the tilted lattice for  $U_1 = 1$  for smaller system  $L = 20$  (lower curves) and  $L = 40$  (upper curves). Different colors correspond to different values of  $F \in [4, 10]$  from dark blue to yellow lines for  $F = 10$ . The initial slow decay of imbalance is ruled by the effective second order tunneling (see text) with time scale proportional to  $F^2$ . This scaling breaks for longer times due to cavity mediated interactions.

To obtain time dynamics of the imbalance (in the absence of disorder) we consider an average over 100 initial separable states. They are not chosen, as in the previous section, by the energy condition but rather we impose that all the initial states have the same dipole moment



$\mathcal{D} = 0$ . Choosing a vanishing dipole moment corresponds roughly to the middle of the energy in Hilbert space shattered [85] spectrum. By taking the same dipole moment we ensure that the initial states belong to the same “sector” in the dynamics. The data in Fig. 5 are presented for a single value of all-to-all interactions  $U_1 = 1$  but for two system sizes  $L = 20$  and  $L = 40$ .  $L = 20$  curves could be also obtained by a standard Chebyshev propagation [86], we present them as a comparison to a typical  $L = 40$  case since tilted lattices with cavity mediated infinite range interactions have not been analyzed before.

For both system sizes the results are quite similar. The initial decay, apart from  $F^2$  scaling, shows some dependence on the system size – initially the decay is slower for the bigger system, while at longer time imbalance for the smaller system saturates faster. This may be attributed probably to the hyper-extensive character of the tilted part of the Hamiltonian – thus for larger systems the approximate conservation of the global dipole shows more strongly – as apparent also from (5). Their long time dynamics, apart from an apparent saturation for significantly non-zero values of the imbalance (revealing localization) is characterized by long period oscillations. Again a careful comparison of both sets of curves reveals that this period reflects the system size. The oscillations, absent for short-ranged Hamiltonian are related to cavity mediated interactions that are system size dependent via  $U_1/L$  term. We believe that they may be related to equally spaced (by integer multiples of  $U_1/L$ ) corrections to energies appearing above in the second order effective tunnelings.

The most important effect of the all-to-all interactions is a significant reduction of the final imbalance values. For short-ranged interactions with  $V = 1$  those values were quite well reproduced by interaction-free analytic expression

$$I_{\text{fin}} = \mathcal{J}_0^2\left(\frac{2J}{F}\right), \quad (6)$$

where  $\mathcal{J}_0(x)$  is the zeroth-order Bessel function thus being above 0.85 for  $F \geq 4$ . For  $U_1 = 1$  the observed imbalance is twice lower indicating that all-to-all interactions play non-trivial role in the dynamics.

As a second example we consider the case of a harmonic potential on top of the lattice,  $h_i = \frac{A}{2}(i - i_0)^2$ , where  $i_0$  denotes the center of the lattice ( $i_0 = 20.5$  for lattice of size  $L = 40$  considered). Such a potential has been considered in [55] where we have found that for short-ranged interactions the system splits into separate regions. While at the center the system delocalizes, clear signatures of localization are observed at the outer regions leading to “phase separation” or the coexistence of localized phases with the ergodic central bubble. This has been attributed to the fact that the local dynamics is governed by a local static field,  $F_{loc} = A(i - i_0)$ , following the first order Taylor expansion of the potential. Indeed soon such a coexistence phenomenon was verified in the quantum simulator experiment [83] where the sys-

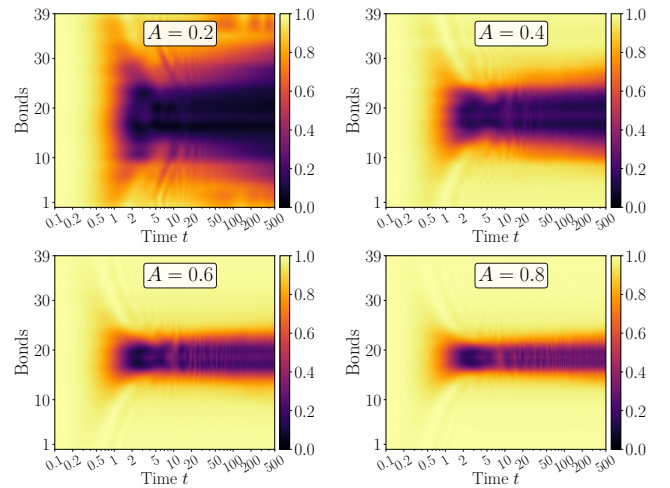


Figure 6. Time dynamics of the local imbalance, (7) for different curvatures,  $A$ , of the harmonic potential placed on top of the lattice. Observe the coexistence of the delocalized central region with outer parts where local imbalance is practically unaffected by dynamics revealing very strong localization.

tem may be described by the long-range-interacting Ising chain.

Figure 6 shows that this is the case also for cavity induced interaction system, (3). To visualize local dynamics we use the concept of local imbalance introduced by us previously [55, 58]. In the spin formulation the local imbalance reads

$$I(i) = 2|\langle S_i^z(0) \rangle \langle S_i^z(t) \rangle + \langle S_{i+1}^z(0) \rangle \langle S_{i+1}^z(t) \rangle|, \quad (7)$$

while for spinless fermions picture one should replace  $S_i^z$  by  $f_i^\dagger f_i - 1/2$ . To be precise  $I(i)$  gives the local imbalance between sites  $i$  and  $i+1$  so it is defined on the bond  $i$  linking these two neighboring sites. As we may observe in Fig. 6 the extend of the dark delocalized region shrinks with the increasing curvature  $A$  of the potential. A careful inspection of the time dynamics reveals the very slow growth of the central region in time even for large  $A$ . This could be mapped to a small non-zero  $\beta$  observed for disordered cases even for large disorder amplitudes and with the slow decrease of the imbalance hidden under pronounced oscillations in Fig. 5. This phenomenon may indicate possible delocalization of the system for very long times. Here we limit the evolution to experimentally feasible times of the order of  $t = 500/J$  [76].

Furthermore, earlier works [55, 58] hinted that for short-ranged interacting systems the transition in space between the localized and delocalized parts of the system depends only on the local effective field value  $F_{loc} = A(i - i_0)$  irrespective of the curvature value  $A$ . To verify this for cavity induced infinite-ranged system, we plot the variations of the long time snapshot of the local imbalance as a function of the local effective field value  $F_{loc}$  in Fig. 7. The collapse of the curves for different values of  $A$  strongly suggests that this is indeed the case also for the infinite-ranged interacting system.

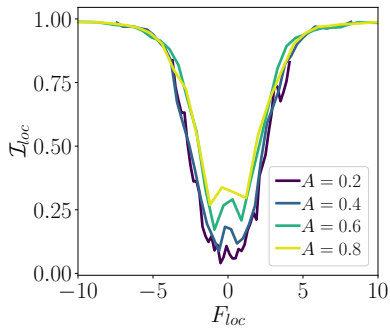


Figure 7. The long time snapshot of the local imbalance as a function of the local effective field value  $F_{loc}$  for the harmonic perturbation of the lattice. Here we consider a system of size  $L = 40$  and different values of the harmonic curvature  $A$ . The long time snapshot has been computed by averaging the data over the time window  $t \in [400/J, 500/J]$ .

## V. DISCUSSION

While MBL is typically considered for short-range interacting systems, the present work shows that strong signatures of non-ergodic dynamics occur for systems with infinite range (all-to-all) interactions. This has been observed for small system sizes [42, 43] amenable to exact localization, we confirm that the similar behavior characterizes larger, experimentally relevant systems. The question arises to what extent this non-ergodic behavior is related to a specific form of all-to-all density-density interactions (compare (1) or (2)) in which no coherent long-range coupling (e.g., long range tunneling) is present. We recall also that the interactions considered are at the border of the condition derived for uniform long range interactions [37, 38, 41] discussed in the Introduction. On the other hand, recent studies of lattice gauge theories indicated [75] that the confinement and the lack of thermalization may occur due to global constraints in the system as those imposed by gauge theories (for recent related reviews see [87, 88]).

We have studied the disordered model of spinless fermions interacting via contact interactions as well as cavity mediated all-to-all forces extending our previous studies to large system sizes. For the standard diagonal disorder we observe that for realistic, experimentally relevant system sizes as well as experimentally achievable coherent evolution times a crossover from delocalized to

localized phase persists for large system sizes. Moreover the corresponding disorder amplitude nicely matches finite size scaling prediction [42].

We have also analyzed localization properties for the all-to-all cavity mediated interactions for disorder-free potentials showing that for moderate  $U_1$  both Stark many-body localization and phase coexistence can be observed both for small and larger, of the order of 100 sites systems. We have considered strongly tilted systems where strong Stark MBL is observed in the absence of infinite range interactions and the Hilbert space has a characteristic shattered character due to approximate conservation of the global dipole moment. Due to large oscillations present in the correlation functions the results were averaged over several initial states corresponding to the same value of the global dipole moment. We must stress again that our conclusions are limited to finite system sizes and finite times corresponding to several hundreds of the tunneling times. Such time scales are relevant for experiments where the coherence times reach at most 700-1000 tunneling times. We observe indications that the systems studied may very slowly delocalize on a much larger time scale but this phenomenon is not possible to be addressed by current tensor network algorithms.

We have considered moderate  $U_1$  values. One may consider what happens if  $U_1$  term dominates the Hamiltonian. This term is diagonal in the Fock site basis and as such is expected to lead on its own, in the limit of  $U_1 \rightarrow \infty$  to Hilbert space fragmentation into parts corresponding to different values of the almost conserved quantity

$$\mathcal{K} = \sum_{i < j} (-1)^{i+j} S_i^z S_j^z = \left( \sum_i (-1)^i S_i^z \right)^2 - \text{constant}. \quad (8)$$

That may lead to additional nonergodic features of the dynamics in this regime, in an analogy to large  $F$  limit.

## ACKNOWLEDGMENTS

The numerical effort was possible thanks to the support of PL Grid infrastructure. The support by National Science Centre (Poland) under project OPUS 2019/35/B/ST2/00034 (J.Z.) is acknowledged.

- 
- [1] I. V. Gornyi, A. D. Mirlin, and D. G. Polyakov, Interacting Electrons in Disordered Wires: Anderson Localization and Low- $T$  Transport, *Phys. Rev. Lett.* **95**, 206603 (2005).  
 [2] D. Basko, I. Aleiner, and B. Altshuler, Metal-insulator transition in a weakly interacting many-electron system with localized single-particle states, *Annals of Physics* **321**, 1126 (2006).

- [3] V. Oganesyan and D. A. Huse, Localization of interacting fermions at high temperature, *Phys. Rev. B* **75**, 155111 (2007).  
 [4] J. M. Deutsch, Quantum statistical mechanics in a closed system, *Phys. Rev. A* **43**, 2046 (1991).  
 [5] M. Srednicki, Chaos and quantum thermalization, *Phys. Rev. E* **50**, 888 (1994).

- [6] R. Nandkishore and D. A. Huse, Many-Body Localization and Thermalization in Quantum Statistical Mechanics, *Annual Review of Condensed Matter Physics* **6**, 15 (2015).
- [7] D. J. Luitz and Y. B. Lev, The ergodic side of the many-body localization transition, *Annalen der Physik* **529**, 1600350 (2017).
- [8] F. Alet and N. Laflorencie, Many-body localization: An introduction and selected topics, *Comptes Rendus Physique* **19**, 498 (2018).
- [9] D. A. Abanin, E. Altman, I. Bloch, and M. Serbyn, Colloquium: Many-body localization, thermalization, and entanglement, *Rev. Mod. Phys.* **91**, 021001 (2019).
- [10] S. Gopalakrishnan and S. Parameswaran, Dynamics and transport at the threshold of many-body localization, *Physics Reports* **862**, 1 (2020).
- [11] J. Z. Imbrie, Diagonalization and many-body localization for a disordered quantum spin chain, *Phys. Rev. Lett.* **117**, 027201 (2016).
- [12] J. Z. Imbrie, On many-body localization for quantum spin chains, *Journal of Statistical Physics* **163**, 998 (2016).
- [13] J. Šuntajs, J. Bonča, T. Prosen, and L. Vidmar, Quantum chaos challenges many-body localization, *Phys. Rev. E* **102**, 062144 (2020).
- [14] R. K. Panda, A. Scardicchio, M. Schulz, S. R. Taylor, and M. Znidaric, Can we study the many-body localisation transition?, *Europhysics Letters* **128**, 67003 (2020).
- [15] P. Sierant, D. Delande, and J. Zakrzewski, Thouless time analysis of anderson and many-body localization transitions, *Phys. Rev. Lett.* **124**, 186601 (2020).
- [16] P. Sierant, M. Lewenstein, and J. Zakrzewski, Polynomially filtered exact diagonalization approach to many-body localization, *Phys. Rev. Lett.* **125**, 156601 (2020).
- [17] D. Abanin, J. Bardarson, G. D. Tomasi, S. Gopalakrishnan, V. Khemani, S. Parameswaran, F. Pollmann, A. Potter, M. Serbyn, and R. Vasseur, Distinguishing localization from chaos: Challenges in finite-size systems, *Annals of Physics* **427**, 168415 (2021).
- [18] J. Šuntajs, J. Bonča, T. Prosen, and L. Vidmar, Ergodicity breaking transition in finite disordered spin chains, *Phys. Rev. B* **102**, 064207 (2020).
- [19] M. Kiefer-Emmanouilidis, R. Unanyan, M. Fleischhauer, and J. Sirker, Evidence for unbounded growth of the number entropy in many-body localized phases, *Phys. Rev. Lett.* **124**, 243601 (2020).
- [20] D. Sels and A. Polkovnikov, Dynamical obstruction to localization in a disordered spin chain, [arXiv:2009.04501](https://arxiv.org/abs/2009.04501).
- [21] D. J. Luitz and Y. B. Lev, Absence of slow particle transport in the many-body localized phase, *Phys. Rev. B* **102**, 100202 (2020).
- [22] P. Sierant, E. G. Lazo, M. Dalmonte, A. Scardicchio, and J. Zakrzewski, Constraint-induced delocalization, *Phys. Rev. Lett.* **127**, 126603 (2021).
- [23] E. V. H. Doggen, F. Schindler, K. S. Tikhonov, A. D. Mirlin, T. Neupert, D. G. Polyakov, and I. V. Gornyi, Many-body localization and delocalization in large quantum chains, *Phys. Rev. B* **98**, 174202 (2018).
- [24] T. Chanda, P. Sierant, and J. Zakrzewski, Time dynamics with matrix product states: Many-body localization transition of large systems revisited, *Phys. Rev. B* **101**, 035148 (2020).
- [25] T. Chanda, P. Sierant, and J. Zakrzewski, Many-body localization transition in large quantum spin chains: The mobility edge, *Phys. Rev. Research* **2**, 032045 (2020).
- [26] P. Sierant and J. Zakrzewski, Can we observe the many-body localization?, [arXiv:2109.13608](https://arxiv.org/abs/2109.13608).
- [27] P. J. D. Crowley and A. Chandran, A constructive theory of the numerically accessible many-body localized to thermal crossover, [arXiv:2012.14393](https://arxiv.org/abs/2012.14393).
- [28] A. Morningstar, L. Colmenarez, V. Khemani, D. J. Luitz, and D. A. Huse, Avalanches and many-body resonances in many-body localized systems, [arXiv:2107.05642](https://arxiv.org/abs/2107.05642).
- [29] D. Sels, Markovian baths and quantum avalanches, [arXiv:2108.10796](https://arxiv.org/abs/2108.10796).
- [30] M. Schreiber, S. S. Hodgman, P. Bordia, H. P. Lüschen, M. H. Fischer, R. Vosk, E. Altman, U. Schneider, and I. Bloch, Observation of many-body localization of interacting fermions in a quasirandom optical lattice, *Science* **349**, 842 (2015).
- [31] J.-y. Choi, S. Hild, J. Zeiher, P. Schauß, A. Rubio-Abadal, T. Yefsah, V. Khemani, D. A. Huse, I. Bloch, and C. Gross, Exploring the many-body localization transition in two dimensions, *Science* **352**, 1547 (2016).
- [32] H. P. Lüschen, P. Bordia, S. Scherg, F. Alet, E. Altman, U. Schneider, and I. Bloch, Observation of slow dynamics near the many-body localization transition in one-dimensional quasiperiodic systems, *Phys. Rev. Lett.* **119**, 260401 (2017).
- [33] H. P. Lüschen, S. Scherg, T. Kohlert, M. Schreiber, P. Bordia, X. Li, S. Das Sarma, and I. Bloch, Single-particle mobility edge in a one-dimensional quasiperiodic optical lattice, *Phys. Rev. Lett.* **120**, 160404 (2018).
- [34] P. Sierant, D. Delande, and J. Zakrzewski, Many-body localization due to random interactions, *Phys. Rev. A* **95**, 021601 (2017).
- [35] P. Sierant and J. Zakrzewski, Many-body localization of bosons in optical lattices, *New Journal of Physics* **20**, 043032 (2018).
- [36] J. Smith, A. Lee, P. Richerme, B. Neyenhuis, P. W. Hess, P. Hauke, M. Heyl, D. A. Huse, and C. Monroe, Many-body localization in a quantum simulator with programmable random disorder, *Nature Physics* **12**, 907 (2016).
- [37] N. Y. Yao, C. R. Laumann, S. Gopalakrishnan, M. Knap, M. Müller, E. A. Demler, and M. D. Lukin, Many-body localization in dipolar systems, *Phys. Rev. Lett.* **113**, 243002 (2014).
- [38] A. L. Burin, Many-body delocalization in a strongly disordered system with long-range interactions: Finite-size scaling, *Phys. Rev. B* **91**, 094202 (2015).
- [39] A. L. Burin, Localization in a random xy model with long-range interactions: Intermediate case between single-particle and many-body problems, *Phys. Rev. B* **92**, 104428 (2015).
- [40] A. O. Maksymov, N. Rahman, E. Kapit, and A. L. Burin, Comment on “Many-body localization in Ising models with random long-range interactions”, *Phys. Rev. A* **96**, 057601 (2017).
- [41] A. O. Maksymov and A. L. Burin, Many-body localization in spin chains with long-range transverse interactions: Scaling of critical disorder with system size, *Phys. Rev. B* **101**, 024201 (2020).
- [42] P. Sierant, K. Biedroń, G. Morigi, and J. Zakrzewski, Many-body localization in presence of cavity mediated long-range interactions, *SciPost Phys.* **7**, 8 (2019).
- [43] P. Kubala, P. Sierant, G. Morigi, and J. Zakrzewski, Ergodicity breaking with long-range cavity-induced

- quasiperiodic interactions, *Phys. Rev. B* **103**, 174208 (2021).
- [44] K. Baumann, C. Guerlin, F. Brennecke, and T. Esslinger, Dicke quantum phase transition with a superfluid gas in an optical cavity, *Nature* **464**, 1301 (2010).
- [45] K. Baumann, R. Mottl, F. Brennecke, and T. Esslinger, Exploring symmetry breaking at the dicke quantum phase transition, *Phys. Rev. Lett.* **107**, 140402 (2011).
- [46] R. Mottl, F. Brennecke, K. Baumann, R. Landig, T. Donner, and T. Esslinger, Roton-Type Mode Softening in a Quantum Gas with Cavity-Mediated Long-Range Interactions, *Science* **336**, 1570 (2012).
- [47] R. Landig, L. Hruby, N. Dogra, M. Landini, R. Mottl, T. Donner, and T. Esslinger, Quantum phases from competing short- and long-range interactions in an optical lattice, *Nature* **532**, 476 EP (2016).
- [48] L. Hruby, N. Dogra, M. Landini, T. Donner, and T. Esslinger, Metastability and avalanche dynamics in strongly correlated gases with long-range interactions, *Proceedings of the National Academy of Sciences* **115**, 3279 (2018).
- [49] U. Schollwöck, The density-matrix renormalization group in the age of matrix product states, *Annals of Physics* **326**, 96 (2011).
- [50] R. Orús, A practical introduction to tensor networks: Matrix product states and projected entangled pair states, *Annals of Physics* **349**, 117 (2014).
- [51] S. Paeckel, T. Köhler, A. Swoboda, S. R. Manmana, U. Schollwöck, and C. Hubig, Time-evolution methods for matrix-product states, *Annals of Physics* **411**, 167998 (2019).
- [52] M. Schulz, C. A. Hooley, R. Moessner, and F. Pollmann, Stark many-body localization, *Phys. Rev. Lett.* **122**, 040606 (2019).
- [53] E. van Nieuwenburg, Y. Baum, and G. Refael, From Bloch oscillations to many-body localization in clean interacting systems, *Proceedings of the National Academy of Sciences* **116**, 9269 (2019).
- [54] S. R. Taylor, M. Schulz, F. Pollmann, and R. Moessner, Experimental probes of stark many-body localization, *Phys. Rev. B* **102**, 054206 (2020).
- [55] T. Chanda, R. Yao, and J. Zakrzewski, Coexistence of localized and extended phases: Many-body localization in a harmonic trap, *Phys. Rev. Research* **2**, 032039 (2020).
- [56] E. V. H. Doggen, I. V. Gornyi, and D. G. Polyakov, Stark many-body localization: Evidence for Hilbert-space shattering, *Phys. Rev. B* **103**, L100202 (2021).
- [57] R. Yao and J. Zakrzewski, Many-body localization in the Bose-Hubbard model: Evidence for mobility edge, *Phys. Rev. B* **102**, 014310 (2020).
- [58] R. Yao, T. Chanda, and J. Zakrzewski, Many-body localization in tilted and harmonic potentials, *Phys. Rev. B* **104**, 014201 (2021).
- [59] W.-H. Li, X. Deng, and L. Santos, Hilbert space shattering and disorder-free localization in polar lattice gases, *arXiv:2103.13780*.
- [60] J. Larson, B. Damski, G. Morigi, and M. Lewenstein, Mott-Insulator States of Ultracold Atoms in Optical Resonators, *Phys. Rev. Lett.* **100**, 050401 (2008).
- [61] C. Maschler, I. B. Mekhov, and H. Ritsch, Ultracold atoms in optical lattices generated by quantized light fields, *The European Physical Journal D* **46**, 545 (2008).
- [62] S. Fernández-Vidal, G. De Chiara, J. Larson, and G. Morigi, Quantum ground state of self-organized atomic crystals in optical resonators, *Phys. Rev. A* **81**, 043407 (2010).
- [63] H. Habibian, A. Winter, S. Paganelli, H. Rieger, and G. Morigi, Bose-Glass Phases of Ultracold Atoms due to Cavity Backaction, *Phys. Rev. Lett.* **110**, 075304 (2013).
- [64] A. E. Niederle, G. Morigi, and H. Rieger, Ultracold bosons with cavity-mediated long-range interactions: A local mean-field analysis of the phase diagram, *Phys. Rev. A* **94**, 033607 (2016).
- [65] K. Rojan, R. Kraus, T. Fogarty, H. Habibian, A. Minguzzi, and G. Morigi, Localization transition in the presence of cavity backaction, *Phys. Rev. A* **94**, 013839 (2016).
- [66] H. Ritsch, P. Domokos, F. Brennecke, and T. Esslinger, Cold atoms in cavity-generated dynamical optical potentials, *Rev. Mod. Phys.* **85**, 553 (2013).
- [67] F. Mivehvar, F. Piazza, T. Donner, and H. Ritsch, Cavity QED with quantum gases: New paradigms in many-body physics, *Advances in Physics* **70**, 1 (2021).
- [68] D. J. Luitz, N. Laflorencie, and F. Alet, Many-body localization edge in the random-field Heisenberg chain, *Phys. Rev. B* **91**, 081103 (2015).
- [69] S. R. White, Density matrix formulation for quantum renormalization groups, *Phys. Rev. Lett.* **69**, 2863 (1992).
- [70] S. R. White, Density-matrix algorithms for quantum renormalization groups, *Phys. Rev. B* **48**, 10345 (1993).
- [71] J. Haegeman, J. I. Cirac, T. J. Osborne, I. Pižorn, H. Verschelde, and F. Verstraete, Time-dependent variational principle for quantum lattices, *Phys. Rev. Lett.* **107**, 070601 (2011).
- [72] J. Haegeman, C. Lubich, I. Oseledets, B. Vandereycken, and F. Verstraete, Unifying time evolution and optimization with matrix product states, *Phys. Rev. B* **94**, 165116 (2016).
- [73] T. Koffel, M. Lewenstein, and L. Tagliacozzo, Entanglement entropy for the long-range ising chain in a transverse field, *Phys. Rev. Lett.* **109**, 267203 (2012).
- [74] M. Fishman, S. R. White, and E. M. Stoudenmire, The ITensor Software Library for Tensor Network Calculations, *arXiv:2007.14822*.
- [75] T. Chanda, J. Zakrzewski, M. Lewenstein, and L. Tagliacozzo, Confinement and lack of thermalization after quenches in the bosonic Schwinger model, *Phys. Rev. Lett.* **124**, 180602 (2020).
- [76] S. Scherg, T. Kohlert, P. Sala, F. Pollmann, B. H. Madhusudhana, I. Bloch, and M. Aidelsburger, Observing non-ergodicity due to kinetic constraints in tilted Fermi-Hubbard chains, *Nature Communications* **12**, 10.1038/s41467-021-24726-0 (2021).
- [77] D. J. Luitz, N. Laflorencie, and F. Alet, Extended slow dynamical regime close to the many-body localization transition, *Phys. Rev. B* **93**, 060201 (2016).
- [78] P. Sierant and J. Zakrzewski, Model of level statistics for disordered interacting quantum many-body systems, *Phys. Rev. B* **101**, 104201 (2020).
- [79] N. Laflorencie, G. Lemarié, and N. Macé, Chain breaking and Kosterlitz-Thouless scaling at the many-body localization transition in the random-field Heisenberg spin chain, *Phys. Rev. Research* **2**, 042033 (2020).
- [80] R. Yao and J. Zakrzewski, Many-body localization of bosons in an optical lattice: Dynamics in disorder-free potentials, *Phys. Rev. B* **102**, 104203 (2020).
- [81] E. Guardado-Sanchez, A. Morningstar, B. M. Spar, P. T. Brown, D. A. Huse, and W. S. Bakr, Subdiffusion and



- Heat Transport in a Tilted Two-Dimensional Fermi-Hubbard System, *Phys. Rev. X* **10**, 011042 (2020).
- [82] Q. Guo, C. Cheng, H. Li, S. Xu, P. Zhang, Z. Wang, C. Song, W. Liu, W. Ren, H. Dong, R. Mondaini, and H. Wang, Stark Many-Body Localization on a Superconducting Quantum Processor, *Phys. Rev. Lett.* **127**, 240502 (2021).
- [83] W. Morong, F. Liu, P. Becker, K. S. Collins, L. Feng, A. Kyprianidis, G. Pagano, T. You, A. V. Gorshkov, and C. Monroe, Observation of Stark many-body localization without disorder, *Nature* **599**, 393 (2021).
- [84] L.-N. Wu and A. Eckardt, Bath-Induced Decay of Stark Many-Body Localization, *Phys. Rev. Lett.* **123**, 030602 (2019).
- [85] V. Khemani, M. Hermele, and R. Nandkishore, Localization from Hilbert space shattering: From theory to physical realizations, *Phys. Rev. B* **101**, 174204 (2020).
- [86] H. Fehske and R. Schneider, *Computational many-particle physics* (Springer, Germany, 2008).
- [87] M. C. Bañuls, R. Blatt, J. Catani, A. Celi, J. I. Cirac, M. Dalmonte, L. Fallani, K. Jansen, M. Lewenstein, S. Montangero, C. A. Muschik, B. Reznik, E. Rico, L. Tagliacozzo, K. Van Acoleyen, F. Verstraete, U.-J. Wiese, M. Wingate, J. Zakrzewski, and P. Zoller, Simulating lattice gauge theories within quantum technologies, *The European Physical Journal D* **74**, 165 (2020).
- [88] M. Aidelsburger, L. Barbiero, A. Bermudez, T. Chanda, A. Dauphin, D. González-Cuadra, P. R. Grzybowski, S. Hands, F. Jendrzejewski, J. Jünemann, G. Juzeliūnas, V. Kasper, A. Piga, S.-J. Ran, M. Rizzi, G. Sierra, L. Tagliacozzo, E. Tirrito, T. V. Zache, J. Zakrzewski, E. Zohar, and M. Lewenstein, Cold atoms meet lattice gauge theory, *Philosophical Transactions of the Royal Society A: Mathematical, Physical and Engineering Sciences* **380**, 20210064 (2022).